Characterizing Spatters in Laser Welding of Thick Steel Using Motion Flow Analysis

Olli Lahdenoja, Tero Säntti, Jonne Poikonen, Mika Laiho, and Ari Paasio

Business and Innovation Development (BID) Unit
Joukahaisenkatu 1 C, Eurocity 2nd Floor
20014 University of Turku, Finland
{olanla,teansa,jokapo,mlaiho,arjupa}@utu.fi

Abstract. Laser welding has become a very important method for industrial manufacturing. Despite of the inherent accuracy of laser welding, the resulting weld quality may still be affected by many dynamic conditions related to the operating parameters and to the properties of the welded material. Methods for monitoring the laser welding process are therefore needed to guarantee consistent manufacturing quality. In this paper, we present a method for characterizing spatters in laser welding of thick steel. Pre-processing and edge detection steps of the proposed algorithm are performed on-line with a very high speed by using a dedicated KOVA1 massively parallel image processing chip, and the actual characterization of the spatters is carried out off-line in Matlab. The methods proposed are simple and efficient, thus also facilitating possible integration of the whole algorithm for on-line processing.

Keywords: Motion flow, Optical flow, Spatters, Laser welding, Thick steel, High-Speed Imaging.

1 Introduction and Background

In the recent years, laser welding has become one of the most used welding methods in industrial applications. This development has been motivated by a number of advantages over traditional methods. These include the increase in productivity due to higher processing speeds and a good suitability for automation, as well as better precision with a smaller heat affected zone. In order to achieve optimal weld quality and welding parameters, monitoring of the laser welding process is required. Automating some of the procedures in both off-line or on-line weld quality inspection can also facilitate the analysis of the phenomena related to the welding process.

Current solutions to monitoring the laser welding process are based on various technologies, including acoustic and optical solutions. The acoustic solutions [1] typically require mechanical contact to the work piece, thus rendering them poorly suited for mass production. Some acoustic monitoring schemes do not require mechanical contact [1], but they are limited by the noisy environment of a factory floor. Optical solutions can be divided in to two categories, ones based on photodiodes and the others based on imaging via CCD or CMOS camera cells.

J.-K. Kämäräinen and M. Koskela (Eds.): SCIA 2013, LNCS 7944, pp. 675–686, 2013.

Monitoring systems based on a discrete photodiodes, which are used for tracking optical emissions from the weld, provide excellent temporal resolution while sacrificing spatial resolution completely. Studies have shown reasonable performance for systems using several photodiodes with different sensitivity ranges (UV, IR or visible light) [2]. Even with multiple detectors, these systems are still limited in their capability to differentiate between all the possible defects that might occur during a weld. These systems also typically require extensive prior knowledge or modeling of the applied welding process in order to extract anomalous behavior from the temporal sensor data.

Weld monitoring systems which apply 2D camera-based imaging allow the detection of process failures by analysing the spatial features of the weld with a higher resolution, which can naturally be combined with the evaluation of transient behavior. In CCD-based implementations the available frame rate of the image sensor is rather limited, and consequently some of the fast dynamic events in a laser weld can not be detected using CCD technology. CMOS-based cameras provide higher image capture speeds, thus alleviating this problem. Using CMOS technology a temporal resolution of well above 10 kFr/s can be achieved while still maintaining sufficient spatial resolution for allowing the detection and discrimination of events that are easily missed by a photodiode based solution.

With the simultaneous availability of sufficient spatial and temporal resolution, several different aspects of the laser weld quality, such a keyhole dynamics and the degree of penetration or different fault generating events can be analyzed. This paper focuses on algoritmic methods for the characterization of material spatter which may lead to degradation of weald seam quality.

In [3] a weld particle or spatter tracking system based on a high-speed CMOS camera was proposed, using frame rates between 1000 and 8000 fps. It was concluded that even a fairly low image resolution between 40x40 and 64x64 pixels is sufficient for the spatial analysis, while a better framerate leads to more robust temporal tracking of events. Another approach for a spatter detection system based on visual laser weld monitoring with a CMOS sensor was proposed in [4], where instead of a normal high-speed camera the Eye-RIS smart camera system [5] based on a focal plane sensor-processor platform was used. The Eye-RIS system allowed some of the image processing to be performed already at the camera.

Laser welding of thick steel with high power laser welding equipment is an emerging application area, which has not yet been extensively studied. In order to be able to adjust the welding parameters correctly, and to examine possibilities of on-line monitoring of the process, quantitative analysis of the spatters is important. In this paper a commercial focal plane processor system was used for image capture and pre-processing the visual laser welding data, while the actual spatter segmentation was at this stage implemented though post-process Matlab simulation. The goal of this study was to develop analysis methods for spatter detection which could later be optimized for online monitoring application through further camera-level processing and e.g. by utilizing a custom high-performance FPGA-based processor platform.

The experiments and monitoring development were carried out in welding scenario of thick steel (>=8mm), which can lead to even more compex material interactions than currently better established sheet metal welding. The method proposed could be used to extend the previously proposed methods for monitoring the welding process with thin material (1mm) [4], in the more demanding scenario of the laser welding of thick steel. In the welding of thick steel an increased occurrence frequency of spatters could be expected to produce an additional difficulty factor.

2 Imaging Devices and Test Setup

2.1 Imaging Hardware

A smart camera prototype system KOVA1 from Kovilta [6] was used to capture and preprocess the welding image data. The core component of the KOVA1 system is a 96x96 pixel resolution massively parallel focal plane array processor IC, which enables on-chip image content analysis both during and after the actual image capture process.

In the focal plane processor architecture each pixel diode sensor is supplemented with compact but programmable analog and digital processing circuitry. This enables e.g. filtering and object segmentation for grayscale images, morphological and logic operations for binary (1-bit) images and multiple image storage to be implemented locally on the pixel level. The pixel cells are also locally connected within the 1st and 2nd neighborhoods in order to facilitate both local image operations as well as regional analysis through asynchnonous propagation of information within the cell array. More information on similar array processor architectures and some examples on the types of possible operations can be found in [7].

Although the spatial resolution of the KOVA1 prototype sensor is limited, this level of resolution has been found to be sufficient for many welding analysis tasks [3]. The main advantage of a smart camera such as KOVA1 or the Eye-RIS vision system [5] which has been previously used for laser welding research [4], is that it not only enables the imaging of the laser welding process, but can also provide a means for analyzing the visual data at very high frame rates, up to tens of kFr/s, depending on the complexity of image analysis algorithms performed on-chip. In the early studies presented in this paper the computation performed on the KOVA1 chip was limited to fairly simple pre-processing and segmentation. However, the optimal approach for facilitating on-line weld quality monitoring is to move as much of the processing to the sensor- or camera level as possible.

The KOVA1 chip is not intended to operate as a regular high speed camera, i.e. for storing high frame-rate video. However, because of the included pixel-level memory, several consecutive 1-bit image frames, which can be the results of on-chip analysis, can be stored within the sensor array at full capture speed and these frame sets can then be read out at the maximum available I/O rate. This allows the evaluation of transient visual events at very high speed. The actual maximum frame rate depends on the lighting conditions and the amount of processing performed within the pixel array.

In the performed laser welding tests the processing capabilities of the KOVA1 system were used first for adaptive capture of the high-intensity laser welding process and then for segmenting the image by on-chip edge detection into 1-bit B/W form, in order to facilitate quick storage of multiple successive image frames.

The maximum frame-rate applied in the performed tests was approximately 25 kFr/s, including the time used for image integration as well as edge detection. Four successive B/W frames were captured at the full image rate in order to test the evaluation of high-speed temporal behavior.

In the adaptive image capture process, the analog processing circuitry within the pixel cells is used to continuously evaluate the regional intensity level with each pixel's neighborhood. The average intensity information is then used to locally reduce the integration time for pixels in very bright regions, while letting the integration process go on for a longer time for the parts of the image with less intensity [7]. This effectively compresses the intensity dynamics of the scene in real time and enables the capture and analysis of image details across very high illumination dynamics, which are typical for the laser welding process. The goal was to take advantage of the secondary visible light emission from the weld to capture both the very bright weld pool area and its lower intensity surroundings, without having to completely filter out the light from the melt pool and use additional (e.g. laser) illumination for the high speed image capture. The challenge was to capture enough detail without either saturating the sensor in the brightest regions or losing too much detail elsewhere. Fig. 1 shows an example of laser welding captured with the KOVA1 camera. On the left a normal sensor operation was used, while on the right the adaptive integration was applied. There is a 1-frame temporal difference between the images, which can be observed from the spatter on the left.

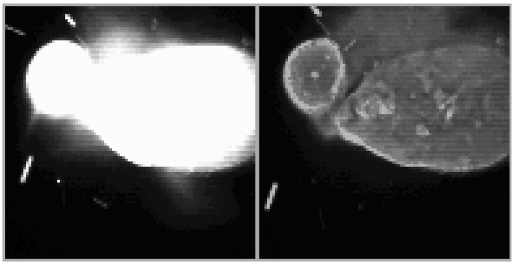

Fig. 1. Normal image (left), adaptive integration (right)

In addition to the adaptive integration, optical filtering with a passband from 700 to 950 nm was applied to filter out the light of the welding laser and plasma. After an image frame was captured, simple segmentation by an edge detection operation was applied. This creates a B/W image which can be efficiently stored at high frame-rates. The 1-bit edge image retains meaningful visual details, such as the shapes and sizes of spatters, for the evaluation of the weld dynamics.

Image edges were obtained by comparing the grayscale value of each pixel to four of its 2^{nd} neighborhood pixels, in two directions both horizontally and vertically, and denoting a pixel as belonging to an edge (black) if the absolute value of any of the differences was larger than a preset (adjustable) threshold value. After the edge detection an isolated pixel removal operation (SMALLKILLER) was performed on the BW image to reduce spurious noise. Fig. 2 shows an example of 2^{nd} -neighborhood edge segmentation performed on the adaptively capture image.

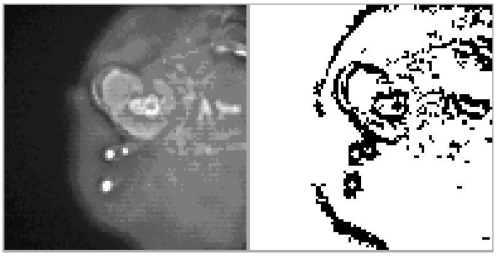

Fig. 2. Grayscale image (left), extracted edge image (right)

2.2 Test Setup

Experimental weld data was obtained from tests performed at the Lappeenranta University of Technology with a 10 kW fiber laser, using 8 or 12 mm steel and a welding speed of 1-3 m/min. The camera was attached to the laser in an off-axis configuration and the size of the captured weld area was approximately 8x8 mm. At this stage the actual welding tests were not set up for the monitoring development in mind and the opportunity to capture welding data was mainly used for the testing and calibration of the image capture process. However, the captured material also enabled the development and testing of algorithms for characterizing the amount of spatter.

In Fig. 3 the imaging setup is shown. The laser beam can also be applied in a scanning mode, where the focal point of the laser beam is moved to the left and to the right from the welding direction during the welding. A high speed air extractor, which pulls towards the plume and smaller spatters (not visible in the image) is placed to the right from the welding direction.

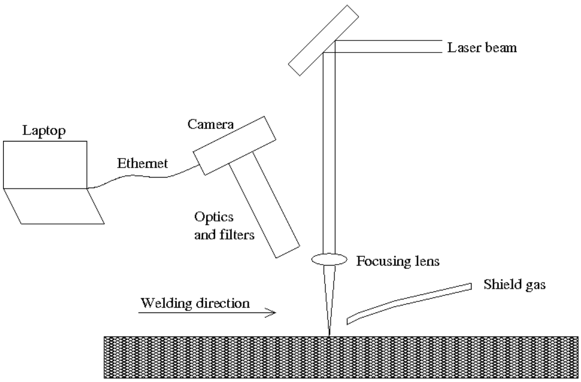

Fig. 3. The welding setup. The imaging part consist of the KOVA1 camera module, connected with Ethernet into a laptop. Optics and filters were used in producing the images in selected wavelength band and spatial size. In the view of the welding direction, shielding gas is injected from the front. Laser beam is focused to the material by using a focusing lens.

2.3 Evaluated Test Sequences

The first test sequence used for spatter characterization was extracted from bead-on-plate welding of 8 mm thick steel with a laser power of 5 kW and a welding speed of 3 m/min. A sequence of image frames was read out and stored through the KOVA1 I/O, each containing 4 consecutive B/W subframes taken without intermediate chip-level I/O. The estimated frame-to-frame rate was approximately 3500 Fr/s between the B/W images. Test sequence 2 was taken with the same welding parameters except for a welding speed of 2m/min. The frame rate in this experiment was approximately 6250 Fr/s due to a shorter image integration time. In order to compare the data to sequence 1 at a similar frame-rate, every other B/W image was skipped in the analysis of test sequence 2. In the welding experiments related to the test sequences 1 and 2, a partial penetration onto the metal was obtained. In the experiments, a caption of 700 frame pairs taken from each of the test sequences was used for further analysis.

3 Image Analysis Applied

3.1 Method and Parameters for Motion Vector Extraction

The extracted test video sequences captured at high-speed were analyzed off-line in Matlab. The sequences consisted of binary edge images captured by the KOVA1 sensor. The binary edge images were analyzed in pairs in order to estimate the motion flow vectors between them and to segment the objects based on their motion [8] [9]. Hence, instead of using both intensity and gradient information for determining the optical flow as in [8], we used only a rough binary image estimate of the gradient to study whether it can give a robust enough motion flow estimate.

The parameters for determining the vectors were set in the following way. Square block windows of size 11 x 11 pixels (+-5 pixels and the center location) were chosen for matching blocks. A search area of size 20x20 pixels was used (+-10 pixel disparity from the borders of the search block). In order to speed-up the image analysis, the motion vectors were extracted using a spacing of 3 pixels in both vertical and horizontal directions. An array of 22 x 22 motion vectors was the result of the motion flow extraction between two frames of size 96 x 96. The location of the upper-leftmost motion vector was centered at position (16,16) and the motion vectors were formed in an uniform grid until the coordinate centered at (79,79), the maximum motion vector length being $10*\sqrt{2}$. The area within half of the search area and half of the block size from the image edges was not considered for starting points of the motion vectors.

The above mentioned parameters were shown to provide robust enough motion vectors, while providing a sufficient velocity interval (motion vector length) in order to capture the small objects traveling at high speed. The image sequences naturally also contained some vapor plume resulting from the high temperature interaction zone between the laser and the metal, which in some cases could be misclassified wrongly as spatters. Fig. 4 (left) shows an example of the extracted motion vectors from the test sequence 2.

The distance metric used in block matching (denoted as D) was defined between block A in previous frame and block B in the successive frame, as $D=\sum_{i,j} XNOR(A_{i,j}, B_{i,j})$, where the indices i and j describe the location of the bits inside the search blocks [9]. To avoid biased motion vectors caused by flat image areas, search blocks of all 0's or all 1's were not considered in matching. In order to promote segmentation of the motion vectors, they were quantized into equally spaced intervals between their (global) maximum length and the minimum length.

3.2 Method for Segmenting Spatters from the Motion Flow Vectors

Motion vectors which were quantized into specific *amplitude levels* were used as inputs for segmentation. Each amplitude level was assigned a separate 22 x 22 sized binary image, describing the neighboring relations between the motion vectors among the motion vector array. A connected component labeling algorithm using 8-neighborhood was then used for each of the extracted binary amplitude level images, in order to segment the spatters according to their amplitude levels. A main requirement for segmenting an object was that at least N (e.g. N>=5) uniform amplitude motion vectors could be assigned to it, while an additional constraint was that they were spatially connected. This allowed the determination of spatter area and size in terms of the number of motion vectors. Also the movement direction of the spatters was determined by quantizing the angles of the individual motion flow vectors. The segmented objects were assigned a dominant movement direction by choosing the most common movement direction angle within the segmented object. In practice, the procedure used could produce relatively accurate segmentation results (see Fig. 4, right).

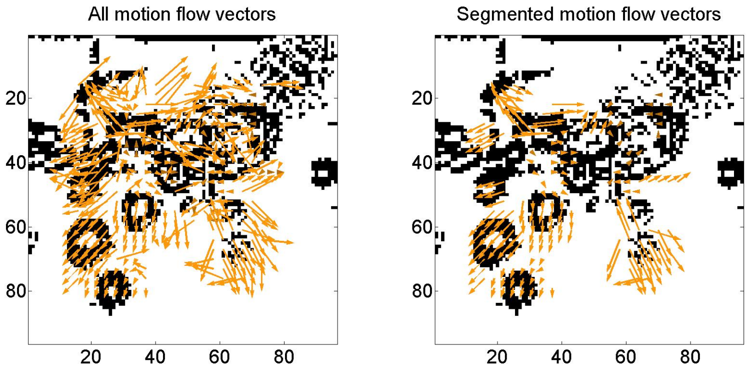

Fig. 4. Extracted motion flow vectors (left), and segmented vectors forming spatters with uniform amplitude (right). At least 5 uniform amplitude motion vectors were required. In this experiment, 15 amplitude levels were used. The example frame was taken from the test sequence 2.

4 Experimental Results

In the following tests, the directions East, South, West and North correspond to the opposite of the welding direction, to the left from the welding direction, to the welding direction and to the right from the welding direction, respectively. The directions of motion are considered within the range of +-45° from the directions East, South, West and North. Ten amplitude levels were used in the experiments of this section. In Fig. 5, the size of the moving objects in terms of number of motion vectors and the dominant movement direction of the spatters are shown by using test sequence 1 (3m/min welding speed). It can be observed that most of the spatters convey to the welding direction (West). Second most frequent movement direction is to the North, which is probably caused by the placement of the air extractor which pulls towards the plume and small objects at a high velocity (it was located in the direction North, i.e. to the right from the welding direction). Otherwise it might be reasonable to assume, that in average, roughly an equal amount of spatters would have been conveyed to the right and to the left from the welding direction. In Fig. 6, the corresponding plot is shown by using the test sequence 2 (2m/min welding speed). An overall increase in the number of spatters can be observed. Otherwise, the results are very similar to the previous test. Also in this test, the spatters were less likely to convey to the direction South. As can be expected, in both tests (Figs. 5 and 6) there is a monotonic tencency that the average number of spatters decrease when increasing N (i.e. the number of motion vectors required for an object).

In Fig. 7, the difference between the number of spatters using the test sequences 1 and 2 is shown. Amplitude level, which can also be used to estimate the velocity of the spatters (since the frame-rate is known) is shown in the x-axis. It can be observed that most the bins are positive, indicating the increase in the number of segmented spatters. Also this test verifies, that the test sequence 2 contained more spatters, although a small difference between the frame-rates of test sequence 1 and test sequence 2 may have affected on the result. In Fig. 7, it can be observed that the increase in the number of spatters was smaller for the very low and the very high object movement velocities (amplitude levels).

Tests were also performed with a scanning laser, where the laser beam moves spatially within a certain limiting interval across the joint. The increase in the number of spatters was verified both by the developed algorithm and visually by a human expert by studying the final weld quality. Imaging frame-rate of approximately 25 kFr/s was used in capturing these sequences. Hence, the methods proposed in this paper could be used as a means for quantitatively characterizing the occurrence frequency and movement of spatters in laser welding in conditions, where the thick metal introduces additional difficulty factor to the analysis of the welding process.

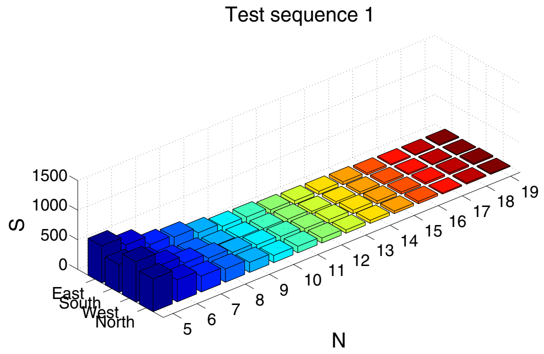

Fig. 5. The number of spatters (S) with respect to their sizes (N) and movement direction. The welding feed direction was to the West. Test sequence 1 was used.

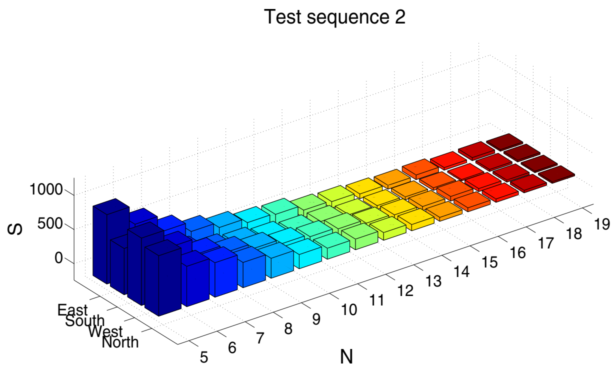

Fig. 6. The number of spatters (S) with respect to their sizes (N) and movement direction. The welding feed direction was to the West. Test sequence 2 was used.

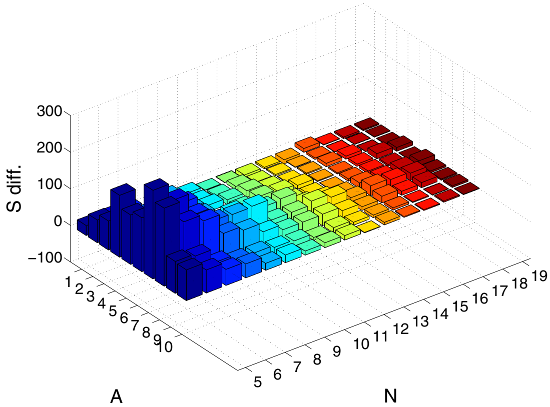

Fig. 7. The difference in number of spatters (S diff.) with respect to the spatter size (N) and amplitude level (A), as S (Test sequence 2) – S (Test sequence 1)

5 Discussion

The proposed algorithm enables the analysis of the spatter characteristics in laser welding. The total energy emitted as spatters from the activity zone could also be estimated. As the estimated time difference between two B/W frames is known (i.e. the frame-rate is known), the approximate velocity of the motion flow within the maximum used amplitude level becomes approximately the maximum motion vector length in pixels times the velocity per one pixel. As a consequence, the maximum spatter velocities captured at the 3500 Fr/s test were at 4.1 m/s, and the corresponding velocities captured at 25 kFr/s were at 29.5m/s (only the effect of the velocity component within the direction of the image plane is considered). Since the number of amplitude levels can be given as a parameter to the algorithm (in Matlab), it might be reasonable to use a larger amount of amplitude levels for higher frame-rates. According to our tests, the segmentation algorithm showed robustness also on various other amplitude level ranges.

In order to further improve the proposed algorithm, the issue of differentiating the spatters more efficiently from the vapour plume should be considered. This could be done by applying a more sophisticated pre-processing step performed on the imaging sensor. As a pre-processing step the roundish blobs only could be selected with the combination of masking the area near the laser beam point of focus [4]. Also a more optimal selection of the wavebands filtered out before the camera could be used to further reduce the amount of plume within the captured images. Analyzing the keyhole dynamics (i.e. the area near the focusing point of the laser beam [4]), could also be incorporated to the proposed method in the case of full-penetration laser welding. Future work also includes considering the possibility to actually track the detected spatters in a longer time-scale.

In [10] a block based motion estimation algorithm was developed on an FPGA for tracking the movement path of a laser welding robot. A total of 1000 3x3 sized blocks were used in a search area of 32x32 to extract the motion flow. The frame rate of 946 fps was obtained. Alternatively the Lucas-Kanade optical flow algorithm was accelerated in [11] by means of a special hardware using the image size of 1024x1024 pixels, while obtaining the processing speed of 1000 fps. In order to segment the motion flow vectors the implementation alternatives of the connected component labeling algorithm should also be studied. In [12] an accelerated FPGA implementation of the connected component labeling reaching the image sizes of 1024x1024 pixels was proposed. Hence, it appears that also the high speed requirement in the view of on-line monitoring (multiple kFr/s) could be met.

6 Conclusions

In this paper, a method for characterizing spatters in laser welding was proposed. The methods proposed are simple and efficient, thus facilitating possible integration of the method for on-line processing also. The proposed method for segmenting spatters was shown to be able to characterize the spatters in terms of their estimated size, movement direction and velocity, and could possibly be used to extend the previously proposed methods in characterizing the spatters in laser welding in the demanding scenario of welding thick steel. In this paper an off-line implementation of the segmentation algorithm was used. Future work includes testing the algorithm with a larger amount of test data. We plan to study the possibilities of applying it to on-line monitoring and extending it by tracking the detected spatters in a longer time-scale.

Acknowledgements. The support from Stefan Grünenwald, Esa Lappalainen, Pertti Kokko and Prof. Antti Salminen from Lappeenranta University of Technology (LUT) is acknowledged. The research was funded by the Academy of Finland project no. 254430.

References

1. Shao, J., Yan, Y.: Review of techniques for On-Line Monitoring and Inspection of Laser Welding. Journal of Physics: Conf. Ser. 15, 101–107 (2005)
2. Norman, P., Engström, H., Kaplan, A.F.H.: State-of-the-art of monitoring and imaging of laser welding defects. In: 11th NOLAMP Conference in Laser Processing of Materials, Lappeenranta, Finland (2007)
3. Jäger, M., Humbert, S., Hamprecht, F.A.: Sputter Tracking for the Automatic Monitoring of Industrial Laser-Welding Processes. IEEE Transactions on Industrial Electronics 55(5), 2177–2184 (2008)
4. Nicolosi, L., Tetzlaff, R., Abt, F., Heider, A., Blug, A., Hofler, H.: Novel algorithm for the real time multi-feature detection in laser beam welding. In: IEEE International Symposium on Circuits and Systems (ISCAS), pp. 181–184 (2012)

5. Rodríguez-Vázquez, A., Domínguez-Castro, R., Jiménez-Garrido, F., Morillas, S., Listán, J., Alba, L., Utrera, C., Espejo, S., Romay, R.: The Eye-RIS CMOS Vision System. In: Casier, H., Steyaert, M., Roermond, A.V. (eds.) Analog Circuit Design: Sensors: Actuators and Power Drives: Integrated Power Amplifiers from Wireline to RF: Very High Frequency Front Ends (2). Springer (2008)
6. http://www.kovilta.fi
7. Laiho, M., Poikonen, J., Paasio, A.: MIPA4k: Mixed-Mode Cellular Processor Array. In: Zarandy, A. (ed.) Focal-Plane Sensor-Processor Chips. Springer (2011)
8. Brox, T., Bruhn, A., Papenberg, N., Weickert, J.: High Accuracy Optical Flow Estimation Based on a Theory for Warping. In: Pajdla, T., Matas, J(G.) (eds.) ECCV 2004. LNCS, vol. 3024, pp. 25–36. Springer, Heidelberg (2004)
9. Lahdenoja, O., Laiho, M.: Regional image correspondence matching method for SIMD processing. In: European Conference on Circuit Theory and Design, pp. 802–805 (2009)
10. Franz, C., Abels, P., Merz, M., Singpiel, H., Trein, J.: Real-Time Process Control by Machine Vision. In: International Congress on Applications of Lasers and Electro Optics, pp. 104–109 (2011)
11. Ishii, I., Taniguchi, T., Yamoto, K., Takaki, T.: High Frame-Rate Optical Flow System. IEEE Transactions on Circuits and Systems for Video Technology 22(1), 105–112 (2012)
12. Benkrid, K., Sukhsawas, S., Crookes, D., Benkrig, A.: An FPGA-Based Image Connected Component Labeler. In: Cheung, P.Y.K., Constantinides, G.A. (eds.) FPL 2003. LNCS, vol. 2778, pp. 1012–1015. Springer, Heidelberg (2003)